Neurochemical Research (2025) 50:181
https://doi.org/10.1007/s11064-025-04432-9

RESEARCH

An Open-Science Computational Model of Organelle Acidification to Integrate Putative Mechanisms of Synaptic Vesicle Acidification and Filling

Emanuele Carnevale Baraglia[1] · Giorgia Fattorini[2,3] · Sandipan Chattaraj[1] · Francesco Pasqualini[1] · Fiorenzo Conti[2,3]

Received: 30 April 2025 / Revised: 13 May 2025 / Accepted: 16 May 2025

Abstract

Organelle acidification has essential implications for the development of degenerative disorders in the brain and heart, but the experimental characterization of these dynamic compartments in native-like contexts is challenging. Computational models can help organize and refine putative mechanisms of organelle acidifications in the same way they helped with brain and heart electrophysiology. Unfortunately, existing models of organelle acidification are not easy to access and operate. Here, we ported the existing model of lysosome acidification into an open-source Python implementation. Furthermore, we hosted this implementation in Google Colab, so everyone with a browser can simulate organelle acidification without a technical background. Finally, we demonstrate how this model can be extended to new organelle types by providing simulations of synaptic vesicle acidification and filling that incorporate different proposed modes of transport and can be fitted to recent experiments.

Keywords Synaptic vesicles · Computational models · Organelle acidification · VGLUT1 · VGAT

Introduction

Synaptic vesicles (SVs) are intracellular organelles responsible for storing and releasing neurotransmitters (NT), key signaling molecules mediating intercellular communication (neuronal and, at least in part, astrocytic) in the central nervous system [1–4]. SVs expressing specific transporters—such as the vesicular glutamate transporter (VGLUT1) [5] and vesicular GABA transporter (VGAT) [6]—selectively accumulate glutamate and γ-aminobutyric acid (GABA) to facilitate excitatory and inhibitory neurotransmission, respectively. Following neurotransmitter release, SVs rapidly re-enter the presynaptic cytoplasm, initially equilibrated with extracellular ionic concentrations but requiring reacidification before efficient neurotransmitter refilling can occur [3]. This acidification primarily depends on the activity of proton pumps (V-ATPases) and chloride/proton exchangers (CLC transporters) [7]. However, the precise roles and interplay of these transport mechanisms remain poorly understood, and conflicting models currently exist [8–11].

Direct measurements of ionic, protonic, and neurotransmitter fluxes within SVs remain technically challenging due to their small size, rapid kinetics, and intracellular localization. Consequently, existing data are collected across in vivo, ex vivo, in vitro, and reconstituted preparations, limiting our ability to integrate findings into a coherent model of SV acidification and loading dynamics. In contrast to neuron electrophysiology, which benefits from

Emanuele Carnevale Baraglia and Giorgia Fattorini contributed equally to this work.

✉ Francesco Pasqualini
francesco.pasqualini@unipv.it

Fiorenzo Conti
f.conti@univpm.it

[1] Synthetic Physiology Lab, Department of Civil Engineering and Architecture, University of Pavia, Pavia, Italy

[2] Department of Experimental and Clinical Medicine, Section of Neuroscience and Cell Biology, Università Politecnica delle Marche, Ancona, Italy

[3] Center for Neurobiology of Aging, INRCA IRCCS, Ancona, Italy

Published online: 05 June 2025

widely accessible computational tools, no equivalent unified computational modeling framework currently exists for SV acidification. Computational models developed originally for self-acidifying organelles, such as lysosomes [12], present a promising starting point. However, these existing lysosomal models are typically embedded in proprietary software, hindering their broader adoption and adaptation by experimental laboratories.

To address these limitations, we developed an accessible, open-source computational modeling framework based on existing lysosomal acidification models, implemented in Python and made freely available via Google Colab. Inspired by recent open-source approaches such as ZeroCostDL4Microscopy [13], our platform democratizes routine computational analyses, enabling broad community access and rapid hypothesis testing. Using this open framework, we adapted lysosomal parameters to reflect SV-specific ionic environments, geometries, and buffering conditions. We explicitly modeled fluxes through key SV transporters—including VGLUT1, VGAT, and CLC-3—using recent experimental kinetic data from preparations closely mimicking physiological conditions. We validated our framework by simulating experimental steady-state SV acidification and neurotransmitter loading data. Finally, we illustrate the flexibility of our approach by comparing alternate transporter models, showcasing how users can easily explore and test competing mechanistic hypotheses and kinetic schemes.

Results

An Open-Source Model of Lysosome Acidification Adapted to Synaptic Vesicles (SV)

Since the primary molecular mechanisms regulating synaptic vesicle (SV) acidification are shared with lysosomes, we began by adapting a previously validated computational model of lysosomal acidification [12, 14]. Lysosomes regulate their luminal pH primarily through three mechanisms (Fig. 1A): proton import via ATP-driven V-ATPase pumps (Fig. 1B), proton-chloride exchange via CLC family antiporters (CLC-7 in lysosomes, Fig. 1C), and passive proton leakage across the lipid bilayer. Together with a powerful but incompletely characterized buffering system, these processes create profoundly non-linear dynamics in luminal pH and membrane potential (ψ). Such non-linear systems can produce counterintuitive behaviors, readily captured through ordinary differential equations (ODEs), similar to those routinely employed in electrophysiological modeling

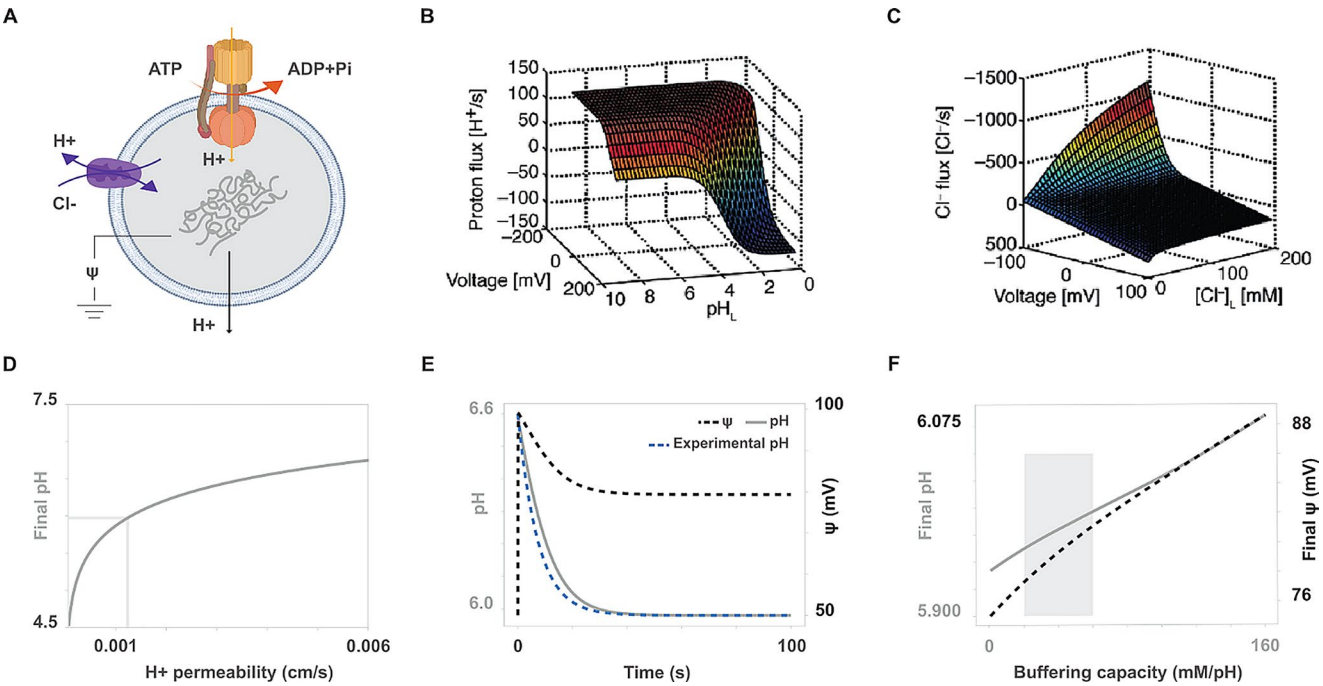

Fig. 1 A computational model of bare SV. Our bare synaptic vesicle model includes [V-ATPase proton pumps, passive proton leak, and CLC-3 chloride/proton exchangers] (**A**), where the kinetics of V-ATPase pumps (**B**) and CLC-3 exchangers (**C**) are directly adapted from the validated lysosome model [12]. The only free parameter remaining in this core model is the passive proton permeability across the vesicle membrane (**D**), which we fitted to experimentally reported steady-state SV acidification levels [11], resulting in accurate simulated time courses for SV pH and membrane potential ψ (**E**). Although SV buffering capacity remains poorly characterized experimentally, our sensitivity analysis (**F**) demonstrates that the steady-state values of vesicular pH and ψ are robust, changing minimally across the buffering capacity range reported in the literature

of neurons and cardiomyocytes. The detailed equations and experimentally validated parameters from lysosomal modeling are fully described in the methods.

To enable broad and open community use, we ported the lysosomal model from its original proprietary software into open-source Python code. Specifically, we implemented our ODE-based model using Python 3.12, leveraging the SciPy library's numerical integration tools [15]. Furthermore, we hosted the complete model within interactive Jupyter notebooks on Google Colab, allowing immediate, browser-based access and interaction without specialized computational infrastructure or commercial licenses. This Colab notebook provides a simple and accessible user interface where simulations can be easily reproduced, parameters adjusted, and hypotheses rapidly tested. Our full implementation can be accessed at: https://colab.research.google.com/drive/1fMFORAUI4OyFXsIHx-d_H8YN3kjAsPT-?usp=drive_link.

To transform the lysosomal model into a bare SV model (Fig. 1A), we integrated prior SV-specific experimental data obtained from electron microscopy and proteomics (Table 1). We adjusted the model to reflect the smaller SV volume (assuming an average radius of 20 nm, consistent with most reports [16]). We also eliminated all ionic fluxes besides the proton leak, reflecting a "bare" vesicle without neurotransmitter transporters. In line with SV proteomics, we included 1.4 V-ATPase [16] and two CLC-3 transporters, adopting their kinetic equations directly from the lysosome model (Fig. 1B–C). With these constraints, only two parameters required estimation: passive proton permeability and buffering capacity. Given the experimental difficulties in characterizing buffering capacity, we adopted a commonly used constant value of 40 µM/pH unit. We then precisely fit the passive proton permeability parameter to match steady-state acidification data from VGAT-knockout vesicles, which lack neurotransmitter transporters. These vesicles equilibrate to a luminal pH of ~5.98 in the absence of VGAT-mediated H^+/GABA exchange [11], providing a reliable experimental target for calibrating the passive leak. The best-fit permeability value of 0.00123 cm/s accurately reproduces this steady-state pH in our simulations (Fig. 1D–E).

Finally, we confirmed the robustness of our results with a sensitivity analysis varying buffering capacity within the physiologically reported range (20–60 µM/pH unit). We found modest changes (~0.16% in pH and ~1.38% in ψ), verifying that our model outcomes are robust against uncertainties in buffering capacity (Fig. 1F). By integrating previously validated equations with explicit SV-specific constraints, we significantly reduced the number of free parameters, avoiding ill-posed fitting scenarios that had challenged earlier models. The steady-state pH and ψ predicted by the model (~5.98 and ~79 mV, respectively) are consistent with independent experimental measurements from reacidifying vesicles [10]. This agreement, along with the model's robustness to buffer variability, supports its use as a reference configuration for subsequent simulations involving neurotransmitter transport (Table 2).

Investigating the Roles of V-ATPase and CLC-3 Via Targeted Scenario Analyses

The modular structure of our computational model makes it straightforward to investigate how specific molecular components contribute individually and interactively to synaptic vesicle acidification. To dissect the roles of V-ATPase and CLC-3 transporters, we systematically simulated scenarios in which each component was selectively removed from the model (Fig. 2).

When both V-ATPase and CLC-3 are active (full model, Fig. 2A), the two transporters initially cooperate to produce

Table 1 Model parameters and values from the literature

Parameter	Value	Reference	Parameter	Value	Reference
Extra/intracellular pH	7.4		*SV diameter*	40 nm	Castorph et al. 2010 [17]
Cytosolic potassium concentration	145 mM	Alberts et al. 2008 [18]	*SV volume*	3.35e-20 L	Spherical geometry
Cytosolic sodium concentration	10 mM	Alberts et al. 2008 [18]	*SV surface area*	5e-11 cm^2	Spherical geometry
Cytosolic chloride concentration	5 mM	Alberts et al. 2008 [18]	*Bilayer capacitance*	1 µF/cm^2	Hille, 2001 [19]
Luminal pH (init) [Lysosome / SV]	7.4 / 6.6	Alberts et al. 2008 [18] / Egashira et al. 2016 [11]	*Buffering capacity*	40 mM/pH unit	Ishida et al. 2013 [12]
Luminal potassium concentration	5 mM	Alberts et al. 2008 [18]	*Osmotic coefficient*	0.73	Kielland, 1937 [20]
Luminal sodium concentration	145 mM	Alberts et al. 2008 [18]	*Water permeability*	0.052 cm/s	Lencer et al. 1990 [21]
Luminal chloride concentration (init)	110 mM	Alberts et al. 2008 [18]	*Partial molar volume of water*	18	Verkman, 2000 [22]
Lysosome chloride permeability	1.2e-5 cm/s	Hartmann and Verkman, 1990 [23]	*Cytoplasmic osmolyte concentration*	290 mM	Ishida et al. 2013 [12]
Number of vATPase per SV	1.4	Takamori et al. 2006 [16]	*Number of VGLUT1 per SV*	9	Takamori et al. 2006 [16]
Number of CLC-3 per SV	2	Takamori et al. 2006 [16]	*Number of VGAT per SV*	1	-

Table 2 Model parameters and values fitted as part of this Article

Parameter	Value	Parameter	Value	Parameter	Value
Proton permeability	0.00123 cm/s	*VGAT GABA transport rate*	65.309 s^{-1}	*VGAT time constant*	13.617 s
GABA efflux time constant	61.869 s	*Maycox VGLUT1 glutamate transport rate*	9.847 s^{-1}	*Maycox VGLUT1 efflux time constant*	188.397 s
Kolen maximum VGLUT1 glutamate transport rate	1.6e4 $s^{-1}V^{-1}$	*Kolen maximum VGLUT1 chloride transport rate*	648.245 $s^{-1}V^{-1}$		

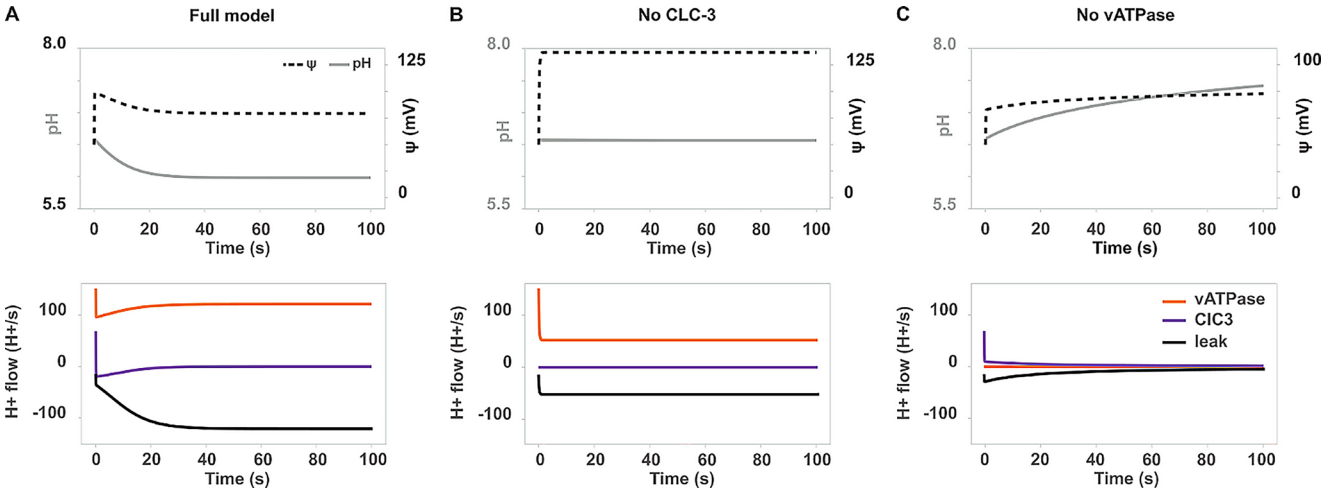

Fig. 2 Role of CLC and vATPase in SV acidification. Our open synaptic vesicle modeling framework allows users to systematically investigate transporter function by adding or removing specific transport mechanisms. Here we demonstrate this flexibility by simulating acidification dynamics under different scenarios (**A**): the full model including V-ATPase and CLC-3, a model without CLC-3 (**B**), and a model without V-ATPase (**C**). Removing CLC-3 transport reveals the critical importance of a chloride counter-ion pathway: the vesicle fails to acidify, and membrane potential collapses, rapidly halting proton pumping by the V-ATPase. Conversely, removing V-ATPase emphasizes the necessity of active proton influx: the vesicle gradually alkalinizes and lacks membrane potential development

rapid SV acidification. Proton pumping by V-ATPase generates a positive membrane potential (ψ) that would quickly inhibit further proton entry. However, CLC-3 transporters reverse direction under increasing ψ, importing chloride ions as counter-ions, dissipating membrane potential, and thus sustaining V-ATPase-driven proton influx and acidification.

Removing CLC-3 transporters (Fig. 2B) prevents acidification entirely. Without chloride influx, membrane potential rapidly reaches inhibitory levels, effectively halting proton import through the V-ATPase pump. This scenario demonstrates that a counter-ion pathway, specifically chloride entry through CLC-3, is critical for sustained proton pumping and effective acidification.

Instead, removing only V-ATPase (Fig. 2C) resulted in a slowly increasing pH response. In this case, the positive membrane potential continuously drives passive proton leakage out of the vesicle, gradually increasing luminal pH. These findings illustrate the essential role of chloride conductance in enabling acidification: without CLC-3, ψ rises rapidly and vATPase activity stalls, preventing pH reduction. This is consistent with longstanding biophysical predictions and with experimental reports that chloride availability accelerates vesicle acidification.

However, our model likely overestimates the absolute dependency on CLC-3, as synaptic vesicles from ClC-3 knockout mice are known to retain some acidification capacity. This discrepancy may reflect the absence of secondary counter-ion pathways (e.g., Na^+/H^+ exchangers or lipid-mediated charge compensation) not yet included in the model. In the vATPase-deleted simulation, the observed proton leakage is not observed experimentally in vesicles exposed to ATP-free buffers. One possible explanation is that CLC-3 becomes inactive or functionally uncoupled when vATPase is not operating. Such regulation could arise through clathrin-mediated inhibition, which is known to affect vATPase activity and could plausibly extend to other transporters [24]. These results exemplify how the model can help generate mechanistic hypotheses that account for both steady-state and dynamic behaviors of vesicular acidification.

Generating Quantitative Hypotheses of SV Filling in GABAergic SV

While some aspects of synaptic vesicle (SV) physiology—such as luminal pH and neurotransmitter content—have been characterized experimentally, detailed kinetic measurements for vesicular neurotransmitter transporters remain scarce. For example, VGAT (the vesicular GABA transporter) plays a central role in determining the acidification and filling dynamics of GABAergic SVs, yet its precise transport kinetics in native conditions are still unknown. However, several key features of VGAT-containing vesicles are experimentally well-established: they equilibrate at a more alkaline resting pH (~6.4) compared to glutamatergic vesicles, and typically contain ~5000 GABA molecules per vesicle [10].

In the absence of detailed kinetic parameters, our model allows us to systematically evaluate how well different simplifying assumptions about VGAT function—such as constant-rate uptake, exponential dependence on time, or inclusion of passive GABA efflux—can reproduce these known properties. In doing so, we treat the model as a tool to test the plausibility of transporter-level assumptions based on their ability to replicate measurable SV state variables.

We first implemented a constant-rate VGAT transporter (Fig. 3A) and found that while this approach supported stable GABA accumulation, it failed to reproduce the transient pH undershoot observed during SV reacidification in GABAergic vesicles (Fig. 3B). This behavior is inconsistent with experimental data from Egashira et al. [11], who reported a rapid initial acidification followed by re-equilibration at a higher resting pH (~6.4). Replacing the constant rate with an exponential transporter rate dependent on time corrected this discrepancy, allowing the model to replicate the biphasic acidification trajectory observed in live neurons (Fig. 3C). However, in the absence of any compensatory efflux, this exponential uptake scheme resulted in unrealistic, unbounded GABA accumulation (Fig. 3D).

To reconcile the acidification dynamics with realistic filling, we added a passive GABA efflux pathway, modeled as non-specific membrane diffusion [25]. This addition yielded a stable dynamic equilibrium that recapitulated both experimentally observed pH and GABA content: ~6.4 for luminal pH (Fig. 3E) and ~5000 GABA molecules per vesicle (Fig. 3F). These values align closely with prior estimates from single-vesicle imaging and quantal content studies [10, 11].

Together, these results illustrate that while full kinetic models of VGAT are still lacking, relatively simple approximations—when grounded in known thermodynamic dependencies and validated against accessible experimental observables—can accurately reproduce key features of GABAergic vesicle physiology. Importantly, the model predicts that passive GABA permeability plays a central role in determining the resting pH of these vesicles, as VGAT must continuously export protons to counterbalance GABA efflux, maintaining a dynamic steady state. This conceptual

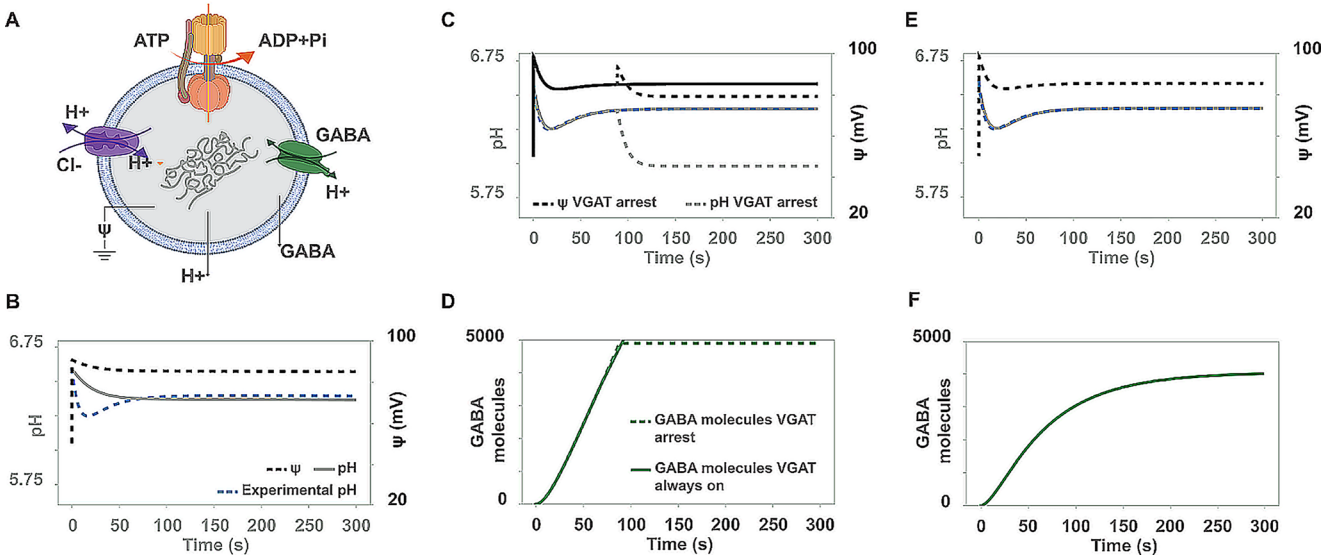

Fig. 3 Testing SV acidification and filling in GABAergic SV. Our open modeling framework readily accommodates neurotransmitter transporters with user-defined kinetic schemes. Here we illustrate this flexibility by modeling GABAergic synaptic vesicles (SVs), incorporating the vesicular GABA transporter (VGAT) into our baseline SV model (**A**). A constant-rate VGAT transporter (**B**) fails to replicate the transient experimental pH undershoot observed experimentally [11]. Adopting a more physiologically realistic exponential rate for VGAT transport (**C**) successfully reproduces the pH undershoot but leads to unrealistic, unlimited accumulation of GABA (**D**). Introducing a passive GABA efflux pathway—representing non-specific neurotransmitter leakage —maintains accurate pH dynamics (**E**) while also limiting neurotransmitter accumulation to physiologically realistic steady-state levels (**F**)

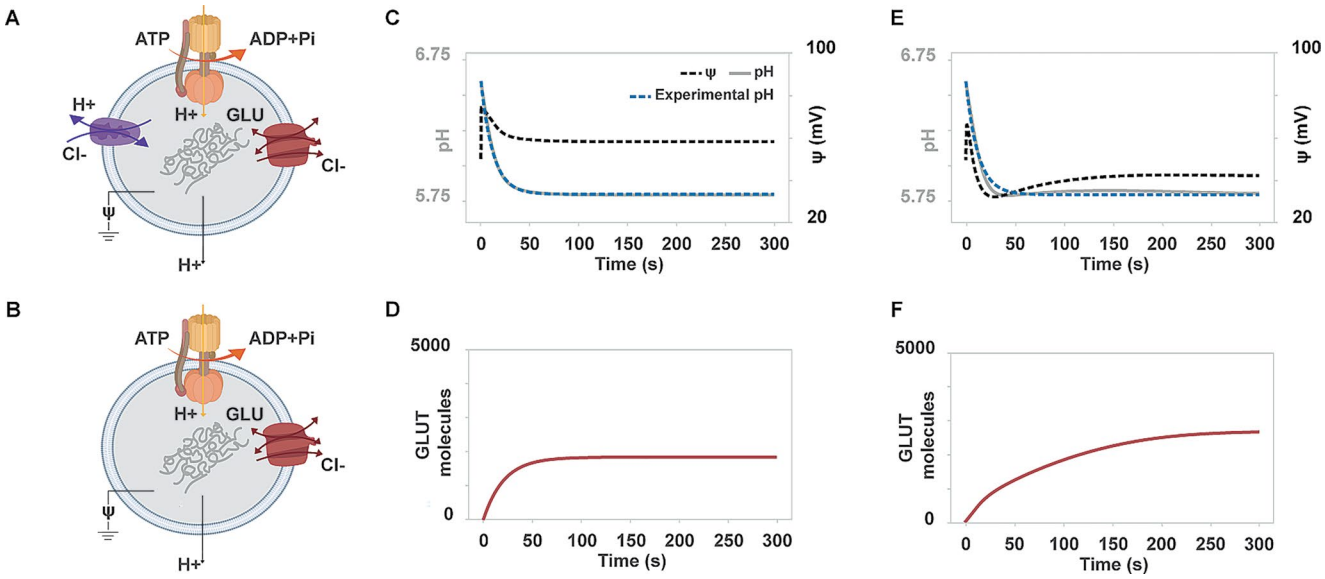

Fig. 4 Glutamatergic SV acidification and filling. Our open modeling framework facilitates direct comparisons between different transporter hypotheses and kinetic mechanisms. Here we illustrate this capability by comparing two prominent models for glutamatergic synaptic vesicles (SVs). The Maycox model (**A**) includes explicit CLC-3 chloride/proton exchangers and allows for potential reverse transport by VGLUT1 [8]. In contrast, the more recent Kolen model (**B**) excludes separate chloride transporters, instead attributing intrinsic chloride permeability directly to VGLUT1 [9]. Simulations using the Maycox model yield monotonic relaxation of membrane potential and accurate acidification kinetics matching available experimental observations (**C**), along with realistic glutamate loading dynamics reaching saturation (**D**). Conversely, the Kolen model predicts distinctly different membrane potential dynamics characterized by a strong initial overshoot followed by a complex biphasic decay (**E**), and results in gradual, non-saturating neurotransmitter accumulation within the modeled timeframe (**F**)

framework provides a tractable starting point for future studies aimed at more detailed kinetic characterization.

Comparative Modeling of Glutamatergic Synaptic Vesicle Acidification and Neurotransmitter Loading

Unlike VGAT, where little is known about kinetic mechanisms, the study of VGLUT1 and glutamatergic synaptic vesicles has progressed rapidly. Earlier models of glutamate uptake—such as those proposed by Maycox et al. [8] in the 1990s—assumed that VGLUT1 functioned as a proton/glutamate exchanger, while ClC-type chloride/proton antiporters (e.g., ClC-3) provided the necessary counter-ion conductance to support sustained acidification. This assumption has been widely adopted in both experimental and modeling work, and aligns with observations that glutamatergic vesicles are highly acidic and maintain a significant membrane potential (ψ).

However, more recent work has prompted a substantial shift in our mechanistic understanding. Kolen et al. [9] demonstrated that VGLUT1 itself exhibits a chloride channel-like conductance mode that is both voltage-gated and independent of glutamate transport. This anion conductance enables charge compensation during H^+-driven glutamate uptake, removing the need for an independent Cl^- transporter. Updated vesicle proteomics studies further support this conclusion by showing that ClC-3 is not consistently detected in VGLUT1-positive vesicles, reinforcing the idea that VGLUT1 alone is sufficient to manage counter-ion flux in these compartments [26].

To explore the implications of these mechanistic differences, we used our modeling framework to simulate and compare the Maycox and Kolen scenarios. In the Maycox-inspired configuration, vesicles include both VGLUT1 and ClC-3 transporters. In this case, we observed monotonic acidification and membrane potential dynamics that matched experimental pH ranges (~5.5–6.0) and yielded realistic transmitter loading (~1800 glutamate molecules), albeit below expected physiological content (Fig. 4C–D). Conversely, in the Kolen-style model—where VGLUT1 supplies both transport and counter-ion conductance—we found a qualitatively different ψ trajectory, with an initial overshoot to ~70 mV followed by a complex biphasic decay (Fig. 4E). Despite producing comparable acidification, the Kolen configuration predicted slower and non-saturating glutamate accumulation over the modeled time frame (Fig. 4F).

These findings illustrate how even relatively small mechanistic revisions—such as replacing ClC-3 with intrinsic Cl^- conductance through VGLUT1—can significantly alter predictions about vesicle membrane potential dynamics, transmitter loading time course, and equilibrium state. Such

predictions can be directly tested in future experiments using voltage-sensitive vesicle dyes or single-vesicle electrophysiology. Moreover, the ability to simulate both transporter configurations using our open-source framework provides a practical tool for resolving such mechanistic uncertainties as new data emerge.

Discussion

We present an open-source, browser-accessible computational framework that simulates the acidification and neurotransmitter loading of synaptic vesicles (SVs) under physiologically grounded assumptions. By porting a validated lysosomal acidification model into Python and deploying it on Google Colab, we provide the research community with an immediately usable and modifiable tool for studying vesicle dynamics. This resource lowers technical barriers for experimentalists and modelers alike, offering a reproducible starting point to explore the nonlinear interplay of proton pumps, ion exchangers, and neurotransmitter transporters in subcellular compartments. As a demonstration of the framework's utility, we applied it to compare acidification and loading dynamics in GABAergic and glutamatergic SVs. These simulations recapitulate key experimental observations: GABAergic vesicles stabilize at higher luminal pH (~6.4) than glutamatergic ones (~5.8), consistent with imaging studies [10, 11]. Mechanistically, we show that steady-state behavior is shaped by the coupling properties of vesicular transporters—VGAT as a proton exchanger and VGLUT1 as an electrogenic antiporter with intrinsic chloride conductance. In GABAergic SVs, dynamic equilibrium arises from a balance between VGAT-driven proton efflux and passive GABA leak. In glutamatergic SVs, the transporter's coupling to membrane potential imposes stronger limits on loading, which may require channel-like counter-ion fluxes as recently described [9]. By making this model openly available, we aim to promote the iterative refinement of mechanistic hypotheses and facilitate data integration across systems and laboratories. The model is not presented as complete but as a flexible scaffold that others can build upon—by testing new transporter kinetics, incorporating additional ion fluxes, or simulating vesicle populations under different physiological or pathological conditions.

Despite its predictive power and close alignment with experimental observables, our current model remains a simplification of the full molecular complexity of synaptic vesicle (SV) physiology. First, we use simplified representations of neurotransmitter transport kinetics—constant-rate or exponential-rate assumptions—in the absence of empirical turnover data. While this approach allows us to fit steady-state luminal pH and content, it does not account for transporter saturation, allosteric regulation, or thermodynamic feedback. Second, passive GABA permeability is modeled phenomenologically, and although consistent with experimental behavior, its absolute magnitude remains loosely constrained. Third, our model assumes fixed transporter copy numbers per vesicle, despite experimental evidence for variability in V-ATPase, VGAT/VGLUT1, and ClC-3 copy numbers across the SV population. Fourth, we simulate isolated vesicles in steady-state conditions, ignoring the effects of endocytosis, cytosolic ion fluctuations, and vesicle trafficking stages (e.g., clathrin-mediated inhibition of vATPase). Extending the model to include stochastic variability in vesicle properties (e.g., transporter counts, proton leak rates) would allow us to simulate the observed heterogeneity in SV pH and content across synapses. Similarly, including the influence of vesicle lifecycle stages (e.g., clathrin coat inhibition of vATPase) would improve accuracy for post-endocytic acidification time courses. Additionally, our current model does not include ion-driven water fluxes or osmotic swelling, which could influence long-term behavior during high-capacity filling. Finally, the model omits alternative counter-ion mechanisms, such as minor K^+ conductance or Na^+/H^+ exchangers, which may provide partial compensation in scenarios where ClC-3 is absent.

These limitations represent natural extensions to the current framework and can be addressed iteratively in future work using the same modular, open approach. The structure and accessibility of our model make it readily extensible to other organelle types—such as lysosomes, endosomes, or dense-core vesicles—that rely on related acidification mechanisms. The modular design allows future users to introduce new transporter mechanisms, test pharmacological perturbations (e.g., protonophores, chloride channel blockers), or simulate specific disease-relevant mutations (e.g., in CLC-3 or V-ATPase subunits). Moreover, because the model is fully implemented in Python and available via Google Colab, it is uniquely positioned to support training, hypothesis generation, and community-driven refinement. Similarly, since our model relies on ordinary differential equations (ODEs), it can be integrated into ODE-based multiscale model of neuron-neuron [27], and neuron-astrocyte networks [28]. We anticipate that as new high-resolution data emerge on transporter stoichiometry, kinetics, and vesicle composition, this model will evolve into a shared platform for simulating subcellular ion dynamics in both health and disease.

Materials and Methods

A Biophysically Accurate Model of Synaptic Vesicles

To model SV acidification, we adapted a framework for pH regulation that was previously validated against endosomes [14] and lysosomes [12] datasets. In this framework, SV are well-stirred compartments separated from the intracellular space by a semi-permeable membrane. The accumulation of protons, cations, and anions determine the SV pH and its membrane potential (ψ) according to:

$$pH = -log_{10}\left({[H^+]_L}/{\beta}\right)$$

$$\psi = \frac{FV}{C_0 S}\begin{pmatrix} \sum_i n_i[cations]_L \\ +\beta\,(pH_C - pH_L) \\ -\sum_j n_j[anions]_L - B \end{pmatrix}$$

Where:

- square brackets indicate molar concentrations;
- the subscripts C and L indicate the cytoplasmic and luminal compartments, respectively;
- n_i and n_j indicate the valences of positive cations and negative anions, respectively;
- F and C_0 are the Faraday constant and the bilayer specific capacitance, respectively.
- V and S are the volume and surface area of the SV, respectively.
- β and B represents the SV buffering capacity (assumed constant) and the negatively charged particles (Donnan particles) that enable the buffering

These equations are valid when the buffering capacity is assumed constant and the impact of osmotic pressures minimal. We made these assumptions based on sensitivity analyses in the earlier studies (and Fig. 1f here) as well as on the paucity of SV-specific datasets for these variables. For a more general treatment, please refer to the endosome and lysosome models. Given the small scale of SV, we retained the explicit treatment of the charge accumulation on the luminal and cytoplasmic side of the membrane. Specifically,

$$\Delta\psi_{TOT} = \Delta\psi - (\psi_C - \psi_L)$$

Where $\Delta\psi_{TOT}$ is the measured potential (positive $\Delta\psi_{TOT}$ will drive cations out of the SV and anions in), and the difference $(\psi_C - \psi_L)$ is evaluated in 50 mV. Importantly, charge accumulation alters the effective intracellular and luminal concentrations of ions felt at the membrane ($[C]_{C,0}$ and $[C]_{L,0}$, respectively):

$$\begin{cases} [C]_{L,0} = [C]_L exp\left(\frac{-zF\Delta\psi_L}{RT}\right) \\ [C]_{C,0} = [C]_C exp\left(\frac{-zF\Delta\psi_C}{RT}\right) \end{cases}$$

Where z is the ion valance, R is the constant of perfect gas, and T is the absolute temperature. To complete the model, we must define how the luminal concentrations of protons and ions can change:

$$\begin{aligned} {d}/{dt}\,[H^+] = & \Im_{H^+}^{pump}(\psi, pH_L) \\ & - \Im_{H^+}^{CLC-3}(\psi, Cl^-) \\ & - \Im_{H^+}^{Leak}(\psi, pH_L) \end{aligned}$$

Annex 1: Modeling Efforts

In contrast to the model described by Ishida et al. [11], we are interested in the neurotransmitters loading of synaptic vesicles and the related pH regulation. Thus, we adapted their model by first removing the passive flow of Na^+, K^+, Cl^- and H_20 through the synaptic vesicle membrane to obtain the so called bare synaptic vesicle model. Then, we introduced GABA and glutamate transporters as described in the following.

The GABA transporter, VGAT, is assumed to be a GABA/H^+ antiporter, with stoichiometry 1:1, whose activity is described by the equation:

$$J_{GABAin} = k_{GABA}\left(1 - e^{-\frac{t}{\tau_{VGAT}}}\right)$$

Where k_{GABA} is the GABA flux [s^{-1}] through the transporter and τ_{VGAT} is the time constant describing VGAT dynamics.

Since GABA is electrically neutral, it is assumed that it can passively leak through the synaptic vesicle membrane. We modeled this efflux with a diffusion equation that depends on the GABA concentration inside the synaptic vesicle and a time constant τ_{GABA}:

$$J_{GABAout} = \frac{VN_A[GABA]}{\tau_{GABA}}$$

Putting these 2 opposing terms together, we got the equation that governs the GABA concentration inside the synaptic vesicle:

$$\frac{d}{dt}[GABA] = \frac{1}{VN_A}\left(N_{VGAT}J_{GABAin} - J_{GABAout}\right)$$

Where V is the synaptic vesicle volume, N_A is the Avogadro constant and N_{VGAT} is the number of VGAT transporters per synaptic vesicle.

Since it is less likely for glutamate (GLUT) to diffuse through the vesicle membrane as it is negatively charged, we modeled the glutamate transporter, VGLUT1, as a bidirectional GLUT/H^+ antiporter, with stoichiometry 1:1, i.e. it can pump glutamate in and protons out and vice versa. The forward operation mode of the transporter pumping glutamate in and protons out is described by a constant rate k_{GLUT} [s^{-1}]:

$$J_{GLUTin} = k_{GLUT}$$

On the other hand, the inverse operation mode depends on the glutamate concentration inside the synaptic vesicle and a time constant τ_{VGLUT}:

$$J_{GLUTout} = \frac{VN_A\,[GLUT]}{\tau_{VGLUT}}$$

Putting these 2 opposing terms together, we obtained the equation that governs the glutamate concentration inside the synaptic vesicle:

$$\frac{d}{dt}\,[GLUT] = \frac{1}{VN_A} N_{VGLUT}\,(J_{GLUTin} - J_{GLUTout})$$

Where N_{VGLUT} is the number of VGLUT1 transporters per synaptic vesicle.

It is also known that VGLUT1 contains a channel through which chloride can flow [29]. We modeled this aspect with the following equation:

$$J_{Cl-VGLUT} = P_{Cl-VGLUT}\frac{U\left([Cl^-]_L e^{-U} - [Cl^-]_C\right)}{1 - e^{-U}}$$

Where $P_{Cl-VGLUT}$ is the permeability [L·(s·mol)$^{-1}$] of this chloride channel and U is the reduced membrane potential defined as:

$$U = \frac{\Delta\,\psi\,F}{RT}$$

Where ΔΨ is the electrical potential across the vesicle membrane, F is the Faraday constant, R is the gas constant and T is the absolute temperature.

Finally, we arrive at the equations for the dynamics of the quantities that are affected by the neurotransmitters' transport, which are Cl^-, H^+, pH and ΔΨ:

$$\frac{d}{dt}\,[Cl^-] = \frac{1}{VN_A}\begin{bmatrix} N_{ClC}\mathcal{J}^{ClC-3}_{Cl^-}(\Delta pH, Cl_L, Cl_C, \Delta\psi) \\ -N_{VGLUT}J_{Cl-VGLUT}\end{bmatrix}$$

$$\begin{aligned}\frac{d}{dt}\,[H^+] =& \frac{1}{VN_A}[N_{pump}\mathcal{J}^{pump}_{H^+}(pH_L, \Delta\psi) \\ &- N_{ClC}\mathcal{J}^{ClC-3}_{H^+}(\Delta pH, Cl_L, Cl_C, \Delta\psi) \\ &- \mathcal{J}^{leak}_{H^+}\left(H^+_L, H^+_C, \Delta\psi\right) \\ &- N_{VGAT}J_{GABAin} - N_{VGLUT} \\ &(J_{GLUTin} - J_{GLUTout})\end{aligned}$$

$$\frac{d}{dt}pH = \frac{1}{\beta}\frac{d}{dt}\,[H^+]$$

$$\Delta\psi = \frac{FV}{C_0 S}\left(\begin{array}{c}\sum\limits_i n_i\,[cation] \\ -\sum\limits_j n_j\,[anion] - [GLUT] - B\end{array}\right)$$

Where β is the buffering capacity, V and S are the synaptic vesicle volume and surface respectively, C_0 is the synaptic vesicle membrane capacitance and B is the luminal concentration of impermeant charges.

The synaptic vesicle model's system of equations is completed by the addition of the equations that describe the dynamics of the neurotransmitter:

$$\frac{d}{dt}\,[GABA] = \frac{1}{VN_A}\,(N_{VGAT}J_{GABAin} - J_{GABAout})$$

$$\frac{d}{dt}\,[GLUT] = \frac{1}{VN_A} N_{VGLUT}\,(J_{GLUTin} - J_{GLUTout})$$

The complete system of equations was implemented in Python and solved using the scipy.integrate.odeint function with default parameters [15].

Parameters were calibrated using experimental data by fitting the model results to the data using lmfit.minimize function with default parameters [30].

Acknowledgements We would like to thank Martina Petrelli for her support in preparing the figures.

Author Contributions E.C.B. Investigation, methodology, data analyses, prepared figures, writing and editing.G.F. Conceptualization, investigation, methodology, data analyses, writing and editing, funding acquisition.S.C. Investigation, methodology, data analyses, writing and editing.F.C. Supervision, conceptualization, editing, funding acquisition.F.P. Conceptualization, investigation, methodology, data analyses, writing, and editing, supervision, funding acquisition.All authors reviewed the manuscript.

Funding Funded by the European Union– Next Generation EU, Mission 4 Component 1 CUP F53D23006790006. We would like to thank Martina Petrelli for her support in preparing the figures.

Data Availability All data and scripts used in this paper can be found on GitHub at the following link: https://github.com/Synthetic-Physiology-Lab/SynapticVesicles. The Google Colab interactive notebooks of the different models can be freely accessed through the following

links: Lysosome model: https://colab.research.google.com/drive/1fMFORAUI4OyFXsIHx-d_H8YN3kjAsPT-?usp=drive_link. bare SV model: https://colab.research.google.com/drive/1EtV4i53Z5IgD20yOeSYRfgFmIQYmw502?usp=drive_link. GABA SV model: https://colab.research.google.com/drive/12dsuN_Rb9_ChnkmmaeYe6zLxL27rClAR?usp=drive_link. GLUT SV model (maycox): https://colab.research.google.com/drive/1IbTQuPaBykC0HO2LEl6o_AIuEbu8cd93?usp=drive_link. GLUT SV model (kolen): https://colab.research.google.com/drive/1XpFQSpKi8KrY1Wut5jfovRHGaXPjgVp0?usp=drive_link.

Declarations

Competing Interests The authors declare no competing interests.

References

1. Sansevrino R, Hoffmann C, Milovanovic D (2023) Condensate biology of synaptic vesicle clusters. Trends Neurosci 46:293–306. https://doi.org/10.1016/j.tins.2023.01.001
2. Südhof TC, Rizo J (2011) Synaptic vesicle exocytosis. Cold Spring Harb Perspect Biol 3:a005637. https://doi.org/10.1101/cshperspect.a005637
3. Chanaday NL, Cousin MA, Milosevic I, Watanabe S, Morgan JR (2019) The synaptic vesicle cycle revisited: new insights into the modes and mechanisms. J Neurosci 39:8209–8216. https://doi.org/10.1523/JNEUROSCI.1158-19.2019
4. de Ceglia R, Ledonne A, Litvin DG, Lind BL, Carriero G, Latagliata EC et al (2023) Specialized astrocytes mediate glutamatergic gliotransmission in the CNS. Nature 622:120–129. https://doi.org/10.1038/s41586-023-06502-w
5. Fremeau RT, Kam K, Qureshi T, Johnson J, Copenhagen DR, Storm-Mathisen J et al (2004) Vesicular glutamate transporters 1 and 2 target to functionally distinct synaptic release sites. Science 304:1815–1819. https://doi.org/10.1126/science.1097468
6. McIntire SL, Reimer RJ, Schuske K, Edwards RH, Jorgensen EM (1997) Identification and characterization of the vesicular GABA transporter. Nature 389:870–876. https://doi.org/10.1038/39908
7. Jentsch TJ, Pusch M (2018) CLC chloride channels and transporters: structure, function, physiology, and disease. Physiol Rev 98:1493–1590. https://doi.org/10.1152/physrev.00047.2017
8. Bacteriorhodopsin drives the glutamate transporter of synaptic vesicles after co-reconstitution (2025) n.d. https://www.embopress.org/doi/epdf/10.1002/j.1460-2075.1990.tb08263.x?_gl=1*1r4hgyf*_up*MQ..*_ga*MTQ4ODIyNTIzOC4xNzQwNjc2NTgz*_ga_D692E1CL8S*MTc0MDY3NjU4Mi4xLjAuMTc0MDY3NjU4Mi4wLjAuMA
9. Kolen B, Borghans B, Kortzak D, Lugo V, Hannack C, Guzman RE et al (2023) Vesicular glutamate transporters are H+-anion exchangers that operate at variable stoichiometry. Nat Commun 14:2723. https://doi.org/10.1038/s41467-023-38340-9
10. Farsi Z, Preobraschenski J, van den Bogaart G, Riedel D, Jahn R, Woehler A (2016) Single-vesicle imaging reveals different transport mechanisms between glutamatergic and GABAergic vesicles. Science 351:981–984. https://doi.org/10.1126/science.aad8142
11. Egashira Y, Takase M, Watanabe S, Ishida J, Fukamizu A, Kaneko R et al (2016) Unique pH dynamics in GABAergic synaptic vesicles illuminates the mechanism and kinetics of GABA loading. Proc Natl Acad Sci 113:10702–10707. https://doi.org/10.1073/pnas.1604527113
12. Ishida Y, Nayak S, Mindell JA, Grabe M (2013) A model of lysosomal pH regulation. J Gen Physiol 141:705–720. https://doi.org/10.1085/jgp.201210930
13. von Chamier L, Laine RF, Jukkala J, Spahn C, Krentzel D, Nehme E et al (2021) Democratising deep learning for microscopy with ZeroCostDL4Mic. Nat Commun 12:2276. https://doi.org/10.1038/s41467-021-22518-0
14. Grabe M, Oster G (2001) Regulation of organelle acidity. J Gen Physiol 117:329–344. https://doi.org/10.1085/jgp.117.4.329
15. Virtanen P, Gommers R, Oliphant TE, Haberland M, Reddy T, Cournapeau D et al (2020) SciPy 1.0: fundamental algorithms for scientific computing in Python. Nat Methods 17:261–272. https://doi.org/10.1038/s41592-019-0686-2
16. Takamori S, Holt M, Stenius K, Lemke EA, Grønborg M, Riedel D et al (2006) Molecular anatomy of a trafficking organelle. Cell 127:831–846. https://doi.org/10.1016/j.cell.2006.10.030
17. Castorph S, Riedel D, Arleth L, Sztucki M, Jahn R, Holt M et al (2010) Structure parameters of synaptic vesicles quantified by Small-Angle X-Ray scattering. Biophys J 98:1200–1208. https://doi.org/10.1016/j.bpj.2009.12.4278
18. Alberts B, Johnson A, Lewis J, Raff M, Roberts K, Walter P (2002) Molecular biology of the cell, 4th edn. Garland Science
19. Hille B (2001) Ion channels of excitable membranes.
20. Kielland J (1937) Individual activity coefficients of ions in aqueous solutions. J Am Chem Soc 59:1675–1678. https://doi.org/10.1021/ja01288a032
21. Lencer WI, Weyer P, Verkman AS, Ausiello DA, Brown D (1990) FITC-dextran as a probe for endosome function and localization in kidney. Am J Physiol-Cell Physiol 258:C309–C317. https://doi.org/10.1152/ajpcell.1990.258.2.C309
22. Verkman AS (2000) Water permeability measurement in living cells and complex tissues. J Membr Biol 173:73–87. https://doi.org/10.1007/s002320001009
23. Hartmann T, Verkman AS (1990) Model of ion transport regulation in chloride-secreting airway epithelial cells. Integrated description of electrical, chemical, and fluorescence measurements. Biophys J 58:391–401. https://doi.org/10.1016/S0006-3495(90)82385-7
24. Farsi Z, Gowrisankaran S, Krunic M, Rammner B, Woehler A, Lafer EM et al (2018) Clathrin coat controls synaptic vesicle acidification by blocking vacuolar ATPase activity. ELife 7:e32569. https://doi.org/10.7554/eLife.32569
25. Hell JW, Edelmann L, Hartinger J, Jahn R (1991) A functional reconstitution of the.gamma.-aminobutyric acid transporter from synaptic vesicles using artificial ion gradients. Biochemistry 30:11795–11800. https://doi.org/10.1021/bi00115a009
26. Taoufiq Z, Ninov M, Villar-Briones A, Wang H-Y, Sasaki T, Roy MC et al (2020) Hidden proteome of synaptic vesicles in the mammalian brain. Proc Natl Acad Sci 117:33586–33596. https://doi.org/10.1073/pnas.2011870117
27. Hines M, Carnevale T, McDougal RA (2022) NEURON simulation environment. In: Jaeger D, Jung R (eds) Encycl. Comput.

Neurosci. Springer, New York, NY, pp 2355–2361. https://doi.org/10.1007/978-1-0716-1006-0_795.
28. Kumar R, Huang Y-T, Chen C-C, Tzeng S-F, Chan C-K (2020) Astrocytic regulation of synchronous bursting in cortical cultures: from local to global. Cereb Cortex Commun 1:tgaa053. https://doi.org/10.1093/texcom/tgaa053
29. Martineau M, Guzman RE, Fahlke C, Klingauf J (2017) VGLUT1 functions as a glutamate/proton exchanger with chloride channel activity in hippocampal glutamatergic synapses. Nat Commun 8:2279. https://doi.org/10.1038/s41467-017-02367-6
30. Newville M, Otten R, Nelson A, Stensitzki T, Ingargiola A, Allan D et al (2024) lmfit/lmfit-py: 1.3.2. https://doi.org/10.5281/zenodo.12785036